

## Plasma Rotation and Wall effects on Resistive Wall Mode in JT-60U

M. Takechi, G. Matsunaga, T. Ozeki, N. Aiba, G. Kurita, A. Isayama, Y. Koide, Y. Sakamoto, T. Fujita Y. Kamada and the JT-60 team

Japan Atomic Energy Agency, Naka, Ibaraki-ken, 311-0193 Japan

e-mail contact of main author: takechi.manabu@jaea.go.jp

**Abstract.** This paper reports the exploration of the RWM onset using co-, near zero, counter plasma rotation profiles in JT60U. This is the first experimental result which demonstrates the dependence of critical RWM onset of plasma rotation and beta on initial plasma rotation with the variation of the angular momentum input and without magnetic braking. In the JT60U with newly ferretic wall installed, it is possible to produce high beta plasma tightly coupled with the wall ( $b/a \approx 1.2$ ) above  $\beta_N > \beta_{N, \text{no-wall limit}}$ . In near-zero plasma rotation, the RWM started to grow at  $\beta_N \approx \beta_{N, \text{no-wall limit}}$  and with finite plasma rotation, the plasma pressure survives up to much higher  $\beta_N$  level than that with small rotation. The observed critical beta onset  $\beta_c$  and the RWM growth rate  $\gamma_{\text{RWM}}$  are discussed along with theoretical predictions using experimentally observed  $q$ -, pressure-, and rotation profiles.

### 1. Introduction

To realize the economical fusion reactor the stabilization of the low  $n$  kink-ballooning mode is necessary because the critical beta of the mode is low for the steady state plasma with high bootstrap current fraction. Kink-ballooning mode can be stabilized by conducting wall. However the stabilized mode, so called RWM, has the slow growth time equivalent to the time constant of the wall. The RWM can be suppressed by the plasma rotation and the active magnetic feedback control. The suppression of RWM by the active feedback control is successfully performed in DIII-D plasmas with large plasma rotation [1]. However, it is considered that the reactor such as ITER rotates hardly at all. Therefore, it is very important to know the characteristics of RWM in the plasma with fairly small rotation. The experiments for RWM physics are performed in the several initial rotation.

#### 1. Installation of Ferritic Steel Tiles and Its Effects on RWM experiment.

Ferritic steel tiles (FSTs) are installed inside the JT-60U vacuum vessel to reduce the toroidal field ripple. The FSTs are set in the low-field-side (LFS) above the outer baffle plates under the TF coils in place of graphite tiles and cover  $\sim 10\%$  of the vacuum vessel surface. Before installing ferritic steel tiles, a few large plasmas reached to ideal beta limit, however it is difficult to exceed it due to lack of NB power. Monte-Carlo simulations considering fully 3-D magnetic field structure using the F3D OFMC code indicate that total absorbed power increases by  $\sim 30\%$  at  $B_T < 2$  T for the large volume configuration close to the wall, which had so far suffered from the large toroidal field ripple. Thanks to increase of NBs deposition power, We successfully achieved high  $\beta_N \sim 4.2$  exceeding ideal limit at  $I_i < 1.2$  and

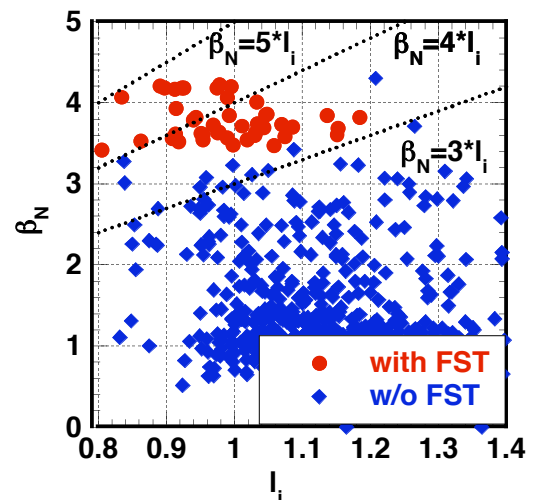


Fig. 1 Achieved  $\beta_N$  as a function of  $I_i$ . redcircle and blue diamonds show the data with and without FSTs

$V_p > 70 \text{ m/s}$  ( $\beta_N \sim 3.4$  w/o FST) Increase net power of  $\sim 3.5$  MW corresponding to 2 tangential beams. It means we can change rotation by one-way tangential NB injection for high beta plasmas.

## 2. High Beta RWM Experiment and stability

Previous RWM experiment was performed on reversed shear plasmas [2]. To increase the achieved beta, we employ the weak shear plasmas. The experiment for RWM is mainly performed on the plasma with the clearance between plasma surface and first wall at low field mid-plane of 20cm, which is equivalent to the ratio of diameter of first wall to plasma of  $\sim 1.2$  (fig. 2). The PNB of  $\sim 20$  MW and the NNB of  $\sim 3$  MW are injected simultaneously into the plasma of  $I_p = 0.9 \text{ MA}$  and  $B_t = 1.58 \text{ T}$ . The plasma has ITB at  $r/a \sim 0.4$  and good pedestal after H mode transition. JT-60U has the NBIs with various directions, such as two co tangential, two counter tangential and seven perpendicular positive NBIs (PNBI). In JT-60U, the net NBI power increases for the large volume plasma due to reduction of ripple loss of energetic particles after installation of ferric steel tiles as the first wall. Therefore, we can perform the high beta ( $\beta_N > 3.5$ ) experiment without some tangential PNBI in order to change the plasma rotation as shown in Fig. 3. Achieved beta is restricted by the  $m=1$  MHD instability. For the co-rotation case, the mode is stabilized for  $\sim 120 \text{ ms}$  and increases as slowly as that for the ctr-rotation (Fig. 4 (a)). On the other hand, for the case of small rotation, the mode is stabilized only for 40ms and increases with relatively fast growth time of  $\tau \sim 10 \text{ ms}$  (Fig. 4 (b)). The mode onset is decided by coherence between two probes. Fig. 5 shows the dependence of the ratio of critical (highest)  $\beta_N$  and  $\beta_N$  at mode onset on plasma rotation at  $r/a = 0.3$ . Larger rotation stabilize the mode for more excessive  $\beta_N$  of mode onset. Before collapse at  $\beta_N \sim 3.6$   $n=1$  MHD mode starts to emerge from  $t \sim 6.5 \text{ s}$  because the coherence between two Mirnov coils separated  $\sim 40$  degree in the toroidal

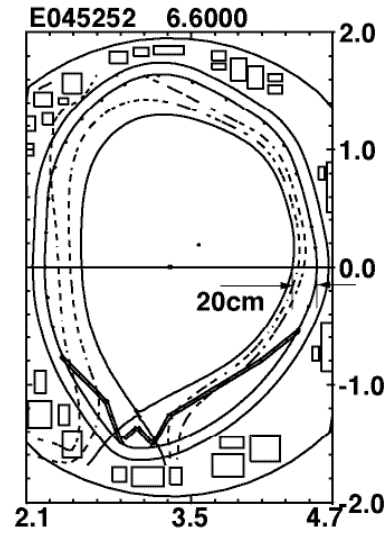


Fig. 2 Poloidal cross-section of the plasma for RWM experiment.

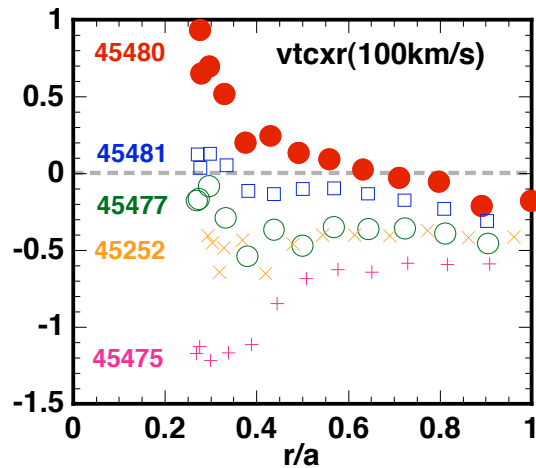


Fig. 3 Toroidal rotation scan for RWM experiment by changing combination of tangential NBIs.

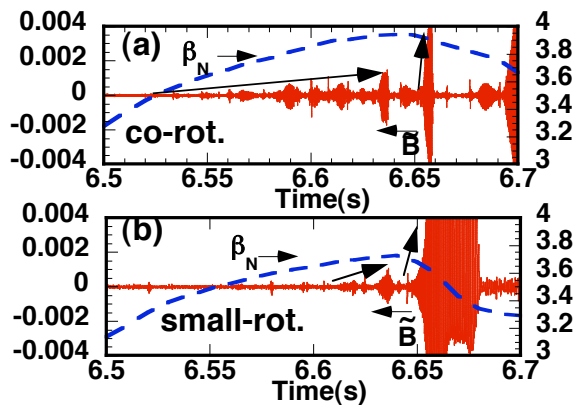


Fig. 4 Temporal evolution of  $\beta_N$  and  $\tilde{B}$  for co-direction of E45480 (a) and no-rotation of E45481 (b).

direction suddenly increase and reach to  $\sim 1$  at this time (Fig. 6 (a)). The main poloidal mode number from magnetic probes is  $m=3$ . The mode is observed by ECE at least from  $r/a \sim 0.1$  to  $0.8$ . Therefore the mode is not localized mode. The mode has a ballooning structure. The mode amplitude increases with slow growth time of  $\tau \sim 20$ ms and then rapidly increases with fast growth time of  $\tau \sim 2$ ms (Fig. 6 (a,b)). The toroidal rotation around  $r/a < 0.4$  in the ITB region decrease after the slow growth mode appeared (Fig. 6 (c)). The rotation at  $r/a > 0.4$  does not change (Fig. 6 (d)). This change of rotation indicate that RWM is coupled with rotation at  $r/a < 0.4$ . The MHD instability is investigated by MARG2D code. The kink-ballooning mode is unstable without first wall. The dominate poloidal component is  $m=1$  as shown in Fig. 7. This mode structure is consistent with interaction of RWM and rotation observed experimentally. This mode is infernal mode and critical beta decrease in the region  $q_{min} < 1.1$  as shown in Fig.8. The experimental minimum  $q$  for high beta case is  $q_{min} \sim 1.08$ . This mode is stabilised by the wall and ideal wall limit reaches  $\beta_N \sim 3.9$  for the plasma at  $d/a = 1.2$ . The critical beta is also affected by the peripheral plasma current. We perform the small current rump down before NB injection to sclope the peripheral current. By this procedure, we achived highest beta  $\beta_N \sim 4.2$ .

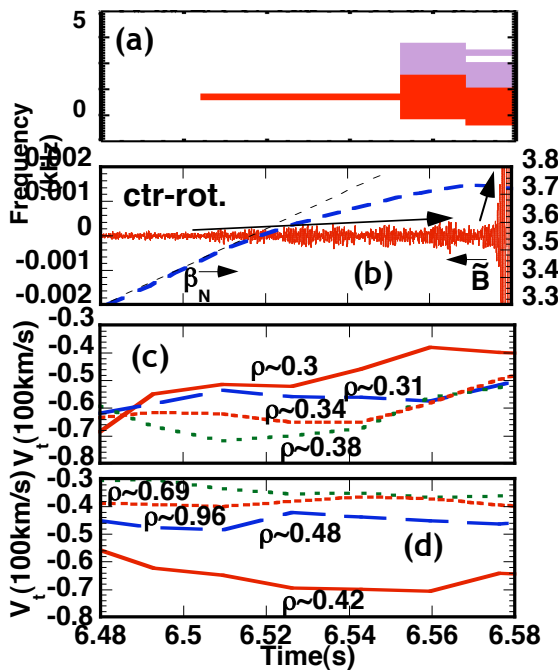


Fig. 6 Temporal evolution of high coherence region (a)  $\beta_N$  and  $B$  (b), toroidal rotation at  $0.3 < r/a < 0.4$  around ITB (c) and  $r/a > 0.4$  (d) for ctr-rotation of E45252.  $V_t$  around ITB decrease after slow RWM appearance.

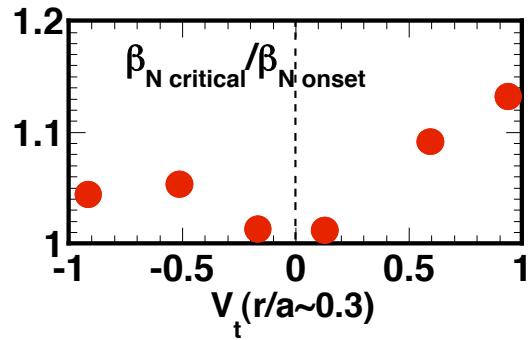


Fig. 5 Dependence of the ratio of critical (highest)  $\beta_N$  and  $\beta_N$  at mode onset on plasma rotation at  $r/a=0.3$ . Larger rotation stabilize the mode for more excessive beta of mode onset.

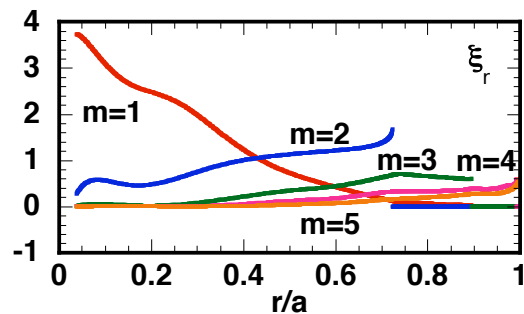


Fig. 7 Displacement of the MHD instability calculated by MARG2D code

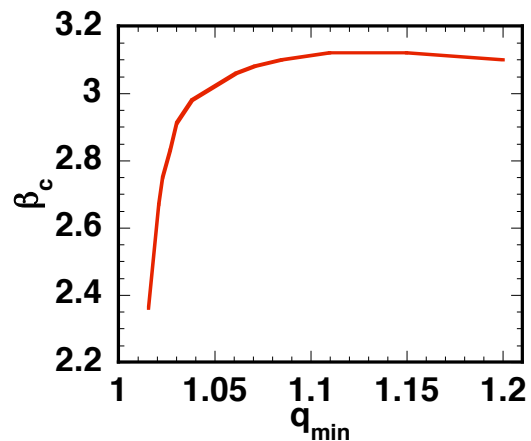


Fig. 8 Critical beta as a function of  $q_{min}$

### 3. High $q_{min}$ RWM Experiment and critical rotation

This infernal mode is strongly affected  $q_{min}$ . Therefore we increase the  $q_{min}$  around 1.5 to investigate the critical rotation.  $\beta_N$  is kept constant and change the tangential NB from ctr-NB to co-NB. In the case of  $\beta_N > \beta_{c, no-wall}$  the plasma disrupted or collapsed. In the case of no change of tangential NB, no disruption or collapse occurred as shown in Fig. 10. To investigate the effect of beta on critical rotation, we change the constant  $\beta_N$ . The critical rotation is  $\sim 10$  kHz and it is corresponding to  $V_t/VA \sim 0.002$ . This value is much smaller than the previous results of DIII-D and JET. It is important that the critical

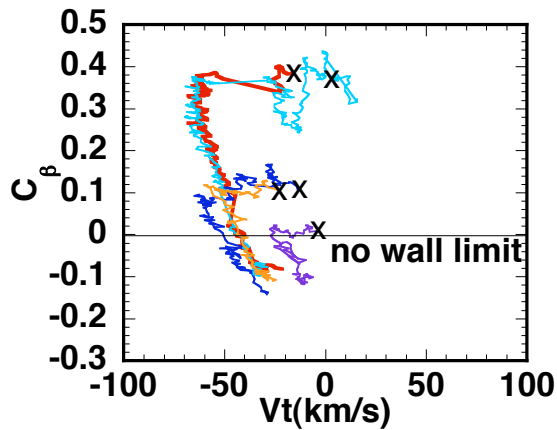


Fig. 11 trajectory of  $V_t$  and  $C_\beta$

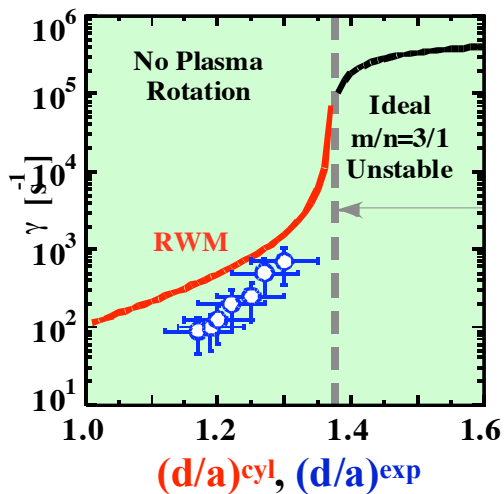


Fig. 12 Dependence of RWM growth rate on  $d/a$ , where  $d$  and  $a$  are diameters of first wall and plasma respectively

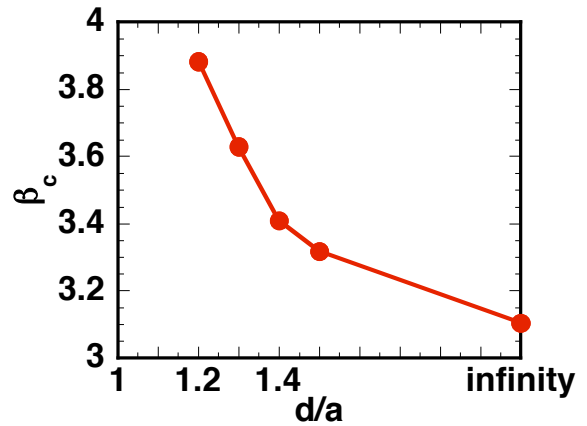


Fig. 9 Critical beta as a function of  $d/a$ .

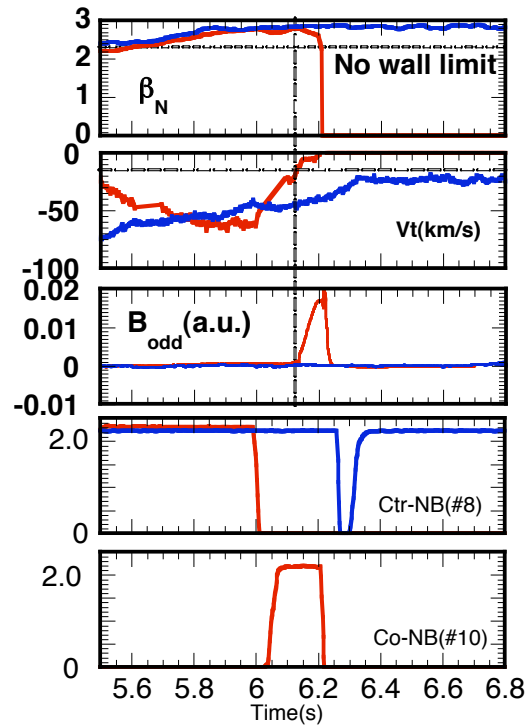


Fig. 10 Waveforms for critical rotation experiment.

rotation does not change by changing beta value.

#### 4. The effect of first wall on RWM stability.

To clarify the wall effect on RWM, we investigated in the JT-60U OH plasma with slightly low beta. The RWM is induced from  $m/n=3/1$  kink mode. The growth rate increase as the plasma is shifted far from first wall. The experimentally obtained growth rate suits

to the value calculated with finn's analytical solution as shown in Fig. 12.

**References**

- [1] M. Okabayashi, et al., Nucl. Fusion **45** (2005) 1715-1731
- [2] S. Takeji, et al., J. Plasma Fusion Res. Vol.78, No.5 (2002) 447-454
- [3] J. M. Finn et. al, Phys. Plasmas **2** 198 (1995)